Desalination and Water Treatment
www.deswater.com

doi: 10.5004/dwt.2023.30101

314 (2023) 110–121
December

Valorization of dam sediments as an adsorbent of a cationic dye, kinetic, isotherm, and thermodynamic studies

Djelloul Addad[a,b,*], Fatiha Mokhtari-Belkhadem[a]

[a]*Laboratory of Functional and Nanostructured Eco-materials, Mohamed Boudiaf University of Science and Technology, Faculty of Chemistry, El Mnaouar, BP 1505, Bir El Djir 31000 Oran, Algeria, email: belkhadem@yahoo.com*
[b]*Natural Substances Valuation Laboratory (LVSN), University Djillali Bounaama of Khemis Miliana, Stat of Thniet El Had, Khemis Miliana, Ain Defla 44225, Algeria, Tel.: (+213) 27556844; email: djelloul.addad@univ-usto.dz*

Received 1 March 2023; Accepted 28 October 2023

ABSTRACT

The objective of this work is to use sediments of an Algerian dam in adsorbing cationic dye, methylene blue (MB) onto aqueous solution, and test their aptitudes in the fixation of organic pollutants. The raw mud sediment (RMS) is characterized using X-ray diffraction, scanning electron microscopy, energy-dispersive X-ray analysis, Fourier-transform infrared spectroscopy, and BET method (Brunauer–Emmett–Teller). The results show that the sediments consist of clay phases; the RMS featured a high surface area of 102.42 $m^2 \cdot g^{-1}$ using the Hang method and 42.39 $m^2 \cdot g^{-1}$ by BET. Adsorption results show that the adsorption kinetics is rapid and adjusted to best fit the pseudo-second-order model. The equilibrium adsorption data analyzed by the Langmuir, Freundlich, and Temkin isotherm models revealed that the isotherm of the solution with initial concentration $C_0 < 100$ $mg \cdot L^{-1}$ obeys to the Freundlich isotherm, and those of concentrations greater than 100 $mg \cdot L^{-1}$ follows the Langmuir model ($R^2 = 0.9919$), equilibrium adsorption 93.72 $mg \cdot g^{-1}$ for an initial concentration of 1,000 $mg \cdot L^{-1}$ was achieved at a temperature of 293 K and pH of 6. The values of the activation parameters such as free energy ($\Delta G°$), enthalpy ($\Delta H°$), and entropy ($\Delta S°$) were also determined. The results indicate that the process of adsorption of MB on the RMS is spontaneous ($\Delta G° < 0$) and exothermic ($\Delta H° < 0$). This study reveals that RMS can be used as an effective low-cost adsorbent of MB from aqueous solutions.

Keywords: Adsorption; Silt sediments; Cationic dye; Langmuir; Freundlich; Methylene blue

1. Introduction

Cationic dyes are widely used in the textile, printing, leather, and paint industry [1,2]. Since the dyes are the contemning of wastewater, they pose an important environmental problem [3,4], such as increased toxicity and chemical oxygen demand of effluents. It has a detrimental effect on photochemical phenomena [5,6]. The methylene blue (MB) dye is not very dangerous but can have harmful effects; the most common side effects are headache, vomiting, confusion, dyspnea, and high blood pressure. More rarely, serotonin syndrome, hemolysis, or allergy can be observed [7,8]. It is necessary to treat these releases before they are discharged into the sanitation network. In this context several processes [9,10] have been used, biological treatment [11], coagulation [12,13], photocatalytic degradation, and electrochemical degradation [14]. The different methods envisaged have disadvantages like incomplete removal, difficulties of implementation, economically are cost and they produce large quantities of by-products of the processing operation with difficult regeneration [15,16]. Additionally, the regeneration of low-cost substances is

* Corresponding author.

not necessary, while that of active carbon is important [17]. In this light, adsorption has emerged as an efficient and cost-effective alternative to conventional contaminated-water treatment facilities. Adsorption is defined as a process wherein a material is concentrated at a solid surface from its liquid or gaseous surroundings. Adsorption has many superior properties compared with other techniques, it reduces the equilibrium concentrations of cations in solution, low initial cost, simplicity of design, ease of operation, insensitivity to toxic substances, and complete removal of pollutants even from their dilute solutions [18]. Thereby encouraging research of materials that are both efficient and cheap, the use of zeolites [19], ion exchangeable resins [20], activated carbons [2,11,21] and aluminum oxide [22] is reported because of their cationic exchange properties in the treatment of organic and metal effluents even in low concentrations [23].

Several researches [24–29] have been directed towards the use of natural materials such as adsorbents and more specifically those based on the clays, because of their availability and their low costs.

Raw mud sediments have the properties of clays compounds; clays have a high adsorption capacity due to their lamellar structure which provides increased specific surface areas. Raw mud sediments exist in large quantities and at a lower cost that can be used as organic effluent adsorbent [30,31]. However, only a limited number of studies on the use of raw mud sediments as an adsorbent have been found in the literature.

Our research is based on the use of the Ghrib dam mud (Algeria) in the removal of the MB cationic dye, used as a model compound for the removal of dyes by adsorption from aqueous solutions, eyesight, its strength on solid adsorbents. The deposit of silty sediments in the dam basin decreases the storage capacity of these dams. Several types of research [32–34] have reported that over time, the initial storage capacity of some dam decreases by 50%.

The removal of these sediments from the dams is a very costly process, this dredging and excavation process leads to considerable volumes of sediment and solid waste that are subject to the environment, it generates the accumulation of a mountain of waste in the landfills. The dredging of a dam can cost the construction of a new dam [35]. It is therefore, important to value this by-product to reduce the cost of the transfer operation on one side and other sides; it is rich in clay minerals favoring the adsorption of organic and mineral effluents.

The aim of the present study is to contribute to the resolution of the environmental and economic problems caused by the dredging of dams. The raw mud sediment (RMS) is an adsorbent therefore at a low cost; it presents a solution to the problems posed.

2. Materials and methods

2.1. Materials

The adsorbent used in this study is the raw mud sediment (RMS) of the Ghrib dam located 100 km west of Algiers (Algeria). We used it in the natural state in the adsorption of MB. The treatment system consists of drying the RMS in the open air for several days until the total elimination of the moisture from the mud. A variant of the particle size range was suspended in freshly distilled water in a 1-L beaker for several hours, and then the mixture was stirred with the addition of a small amount of hydrogen peroxide (30%) (H_2O_2) solution to eliminate existing organic substances at the level of the crude mud until all effervescence has ceased [36]. Then treated with hydrochloric acid to attack carbonates. Several washing were carried out on the recovered mud and then dried in the oven at 105°C. The material thus obtained is crushed, sifted in several grain sizes, and stored for use as an adsorbent in the crude state of the MB dye [26].

The adsorbents used are characterized by X-ray diffraction (XRD; Type of the diffractometer: PANALYTICAL PW-3710, the monochromatic stripe used: FeKα, over the range of 2θ = 10°–80° and a low speed of rotation with a pitch of 0.02°/s), scanning electron microscopy-energy-dispersive X-ray (SEM-EDX) analyzes by (Bruker Nano GmbH, Germany) was used to observe the surface morphology of composites. Fourier-transform infrared spectroscopy (FTIR) analysis of raw mud sediments were performed using PerkinElmer 983 G-IR spectrometer in the range of 4,000–400 cm^{-1}.

Their specific surfaces are determined by the adsorption of MB and by the BET method (Brunauer–Emmett–Teller) (Micromeritics ASAP 2000), nitrogen adsorption–desorption at 77°K.

The adsorbate used is methylene blue (MB, or tetramethylthionine chloride) [15], a cationic dye with a molecular mass of 373.9 $g \cdot mol^{-1}$ of crude chemical formula $C_{16}H_{18}ClN_3S \cdot 3H_2O$, and water solubility exceeding 100 $mg \cdot L^{-1}$ [31]. It is in the form of a rectangle parallelepiped of dimensions 17.0 Å × 7.6 Å × 3.25 Å [5,37–39].

- It is an organic pollutant encountered in wastewater from various industries: textiles and paper, pharmaceuticals, food processing.
- It is a reference molecule for testing adsorbent materials (one of the most encountered in the literature), which makes it possible to compare the results obtained in this work with those from the literature.
- In addition, research carried out on the destruction of organic pollutants in the aqueous phase is most often interested in compounds refractory to biological treatment, such as aromatic compounds.

The study of the visible UV spectrum of MB was performed at wavelengths between 200 and 1,100 nm. The device used is a HACH DR3900 type spectrophotometer. This analysis allowed us to determine the wavelength that corresponds to the maximum absorbance λ_{max} = 664 nm. The latter was used to determine the equilibrium concentrations of MB (C_e) in the rest of the work.

2.2. Methods

All of the solutions used for adsorbate (the MB) are prepared from a concentration solution (1,000 $mg \cdot L^{-1}$). The study was carried out in a batch process, in a set of Erlenmeyer flasks (250 mL) with 50 mL of MB solution. About 0.5 g

(64–80 μm) of sediment adsorbents was added, mixed, and placed in a water-batch of MB with known initial concentration for limited durations. At equilibrium, the final concentration in the flasks is determined using a UV spectrophotometer at the wavelength λ_{max} already determined.

The amount of MB adsorbed at equilibrium (Q_e) and at time t, q_t (mg·g^{-1}) on the adsorbent mud were calculated using Eqs. (1) and (2), respectively:

$$Q_e = \frac{C_0 - C_e}{m} V \quad (1)$$

$$q_t = \frac{C_0 - C_t}{m} V \quad (2)$$

where Q_e and q_t (mg·g^{-1}): the amount of MB adsorbed at equilibrium and at time t; C_0 and C_e (mg·L^{-1}): initial and equilibrium concentrations of MB; V (L): volume of solution of MB; m (g): the mass of the adsorbent RMS; C_t (mg·L^{-1}): the concentration at any time t of the dye.

3. Results and discussions

3.1. Characterization of the adsorbent

3.1.1. X-ray diffraction characterization

The results obtained by XRD are shown in Fig. 1A and B. The results reveal that the raw mud sediment consists of illite, halloysite and, impurities such as quartz [40], organic matter, and carbonates (calcite, magnetite, or dolomite) [41,42], seen, that the mud was not the seat of a prior purification and to clarify the nature of the clay phases, a specific analysis was performed on the particle size fraction less than 2 μm. These analyses are made on three oriented blades (Fig. 1B):

- First corresponds to the raw material;
- Second blade is heated to 450°C for 2 h to characterize the mineral at 7 Å whose diffraction peaks are disappearing or greatly attenuated at this temperature;
- Third blade is saturated by ethylene glycol vapors to highlight the swelling clay phases of the smectites type [43].

Thus, it can be argued that the clay fraction consists of smectites (montmorillonite clay) [44,45], halloysite, illite, and chlorite [46,47]. Moreover, our silt contains impurities such as quartz (d = 7.11221 Å), calcite (d = 9.88153 Å) [15,31,48].

3.1.2. SEM and FTIR analyses

The surface of the sample was characterized by SEM. The SEM species can easily enter into the pores of the sediment (Fig. 2). The raw mud displayed a rigid, flat, and homogeneous surface, without visible pores [49]. The energy-dispersive X-ray analysis (EDX) analysis of the beads confirmed the presence of Ca, O, Al, and Si in large proportion, but F, Fe and, Na in small proportion. This confirms the presence of clay minerals in the raw mud sediment (RMS).

The FTIR spectrum revealed (Fig. 3A) band at 3,697.86 cm^{-1} corresponding to the OH stretching vibrations of the RMS surface [14]. The interlayer absorption capacity of water is confirmed in the RMS sample, by the absorption band at 3,607.86 cm^{-1} which is more intense in sample MB with RMS and appears at 3,617.59 cm^{-1}. This explains the more accentuated anion exchange property of this sediment. The bands characteristic of stretching vibrations of Si–O are shown at 1,099 and 1,035 cm^{-1}, the band appears at 909.05 cm^{-1} is due to the Al–OH groups of the RMS. In addition, the bands appear at 875.71 and 798.57 cm^{-1} are attributed to the Si–O–Al stretching vibration [13]. In the

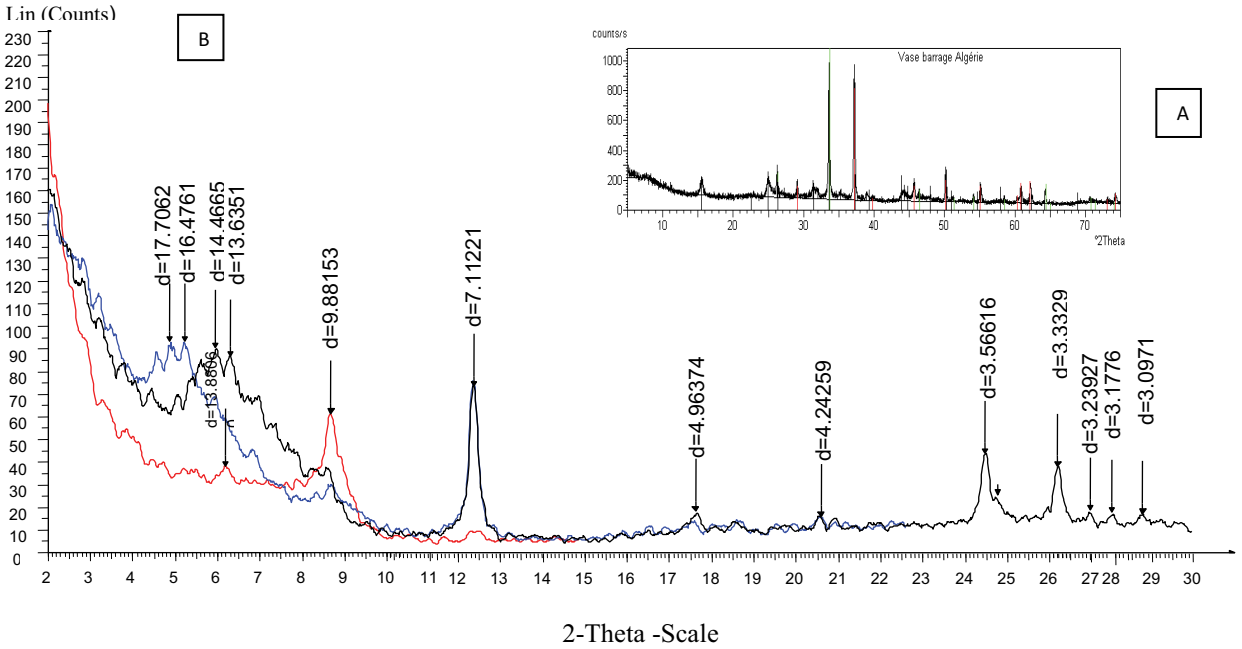

Fig. 1. Diffractogram of the raw mud sediment dam (Algeria).

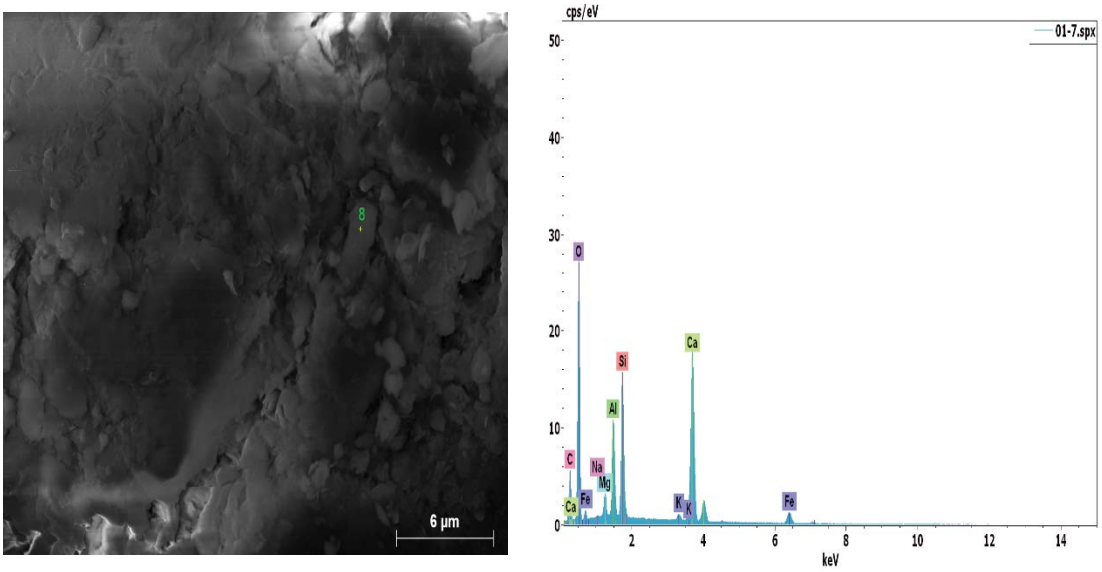

Fig. 2. Scanning electron microscopy images and energy-dispersive X-ray analysis patterns of raw mud sediments.

FTIR analysis of adsorbent loaded with MB (Fig. 3B), band appears at 1,638.04 cm^{-1}, which is characteristic of aromatic cycle of MB cationic dye and a large band at 3,425.84 cm^{-1} corresponding to the stretching vibration band S–OH due to the fixation of MB with RMS.

3.1.3. Specific surface measurements

The methods of determining the specific surface are generally based on the adsorption of polar liquids such as water [50]. The adsorption of MB is one of the common methods for estimating the specific surface area of some smectites [51–54]. Kahr and Lorenz Meier have shown that the specific surface method using MB is more accurate for montmorillonite than for other phyllosilicate [55]. The results of determination of the specific surface with different methods are listed in (Table 1). It clearly appears that the specific surface determined by the method of Hang 102.42 ($m^2 \cdot g^{-1}$) presents the highest value. The study carried out by Dali-Youcef et al. [31] on the mud of the Fergoug dam (Algeria) showed that the specific BET surface of this mud S_{BET} is 54.58 $m^2 \cdot g^{-1}$ with a pH of 9.9.

The specific surface determined by the three methods is different, the specific surfaces of the mud defined by the method of Kahr [38–39,52] and by the method developed at the University of Laval Canada [53] are close, which indicates that our mud contains a large percentage of smectites, in line with the results of XRD (Fig. 1A and B). The specific surface determined by BET method (Lecloux [54]) is the smallest, which confirms that this method determines the external specific surface [37].

3.1.4. Zero charge point pH_z

The zero charge point of dam sediments was determined by the solid addition method. It corresponds to the intercept point of the final pH curve with that of the initial pH. The pH_z of the dam sediments is 8.0 (Fig. 4).

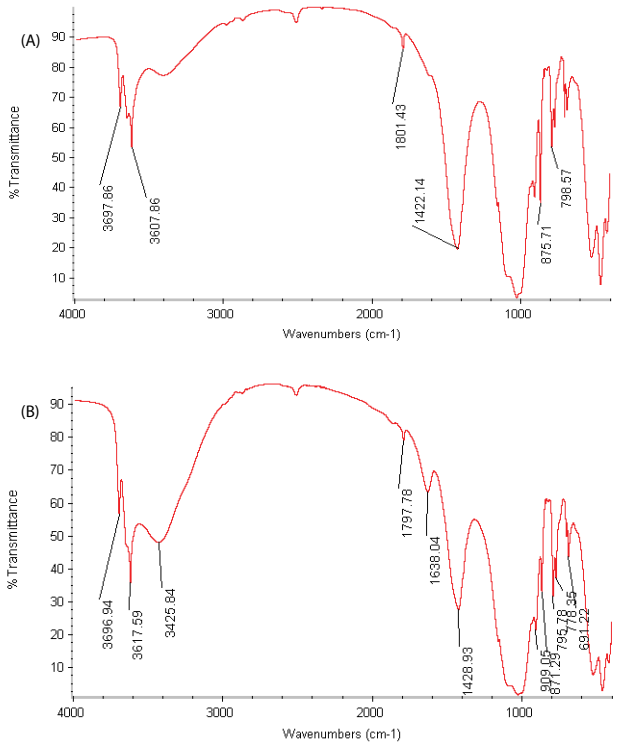

Fig. 3. Fourier-transform infrared spectroscopy spectrum of raw mud sediment (A) and adsorbent loaded with methylene blue (B).

3.2. Adsorption study

3.2.1. Effect of adsorbent dose

This study enabled us to determine the ratio (R) optimum adsorbent/adsorbate and the fraction of the corresponding adsorbent diameter. While taking into consideration, adsorption effect of initial concentration. The effect

Table 1
Specific surface of the sediments

Methods used	S_s ($m^2 \cdot g^{-1}$)
Method of Hang	102.42
Method of Kahr	89.17
Method of Laval	90.46
Brunauer–Emmett–Teller	42.39

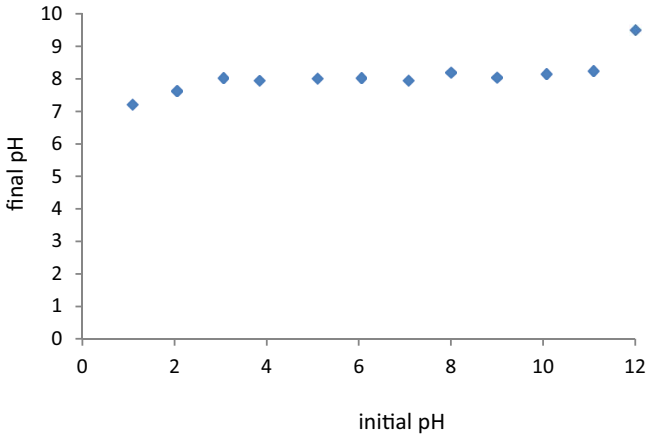

Fig. 4. pH at the point of zero charge pH_z of raw mud sediments.

of adsorbent dose was varied in the range of 2 to 10 $g \cdot L^{-1}$ and was used for the adsorption experiments. The results are given in (Fig. 5). We note that the removal rate of MB ions increases gradually with increasing adsorbent dose. It increases from 10.46 to 78.05 $mg \cdot g^{-1}$. This rise in removal rate of MB ions could be due to availability of more surface area and functional groups. The adsorbent dose of 8 $g \cdot L^{-1}$ and a diameter of grains of ($62 < d < 80$ μm) is considered as equilibrium value and was taken as the optimal adsorbent dose for the subsequent experiments.

3.2.2. *Effect of pH*

The adsorption is dependent on pH, and temperature of the solution. Solution pH affects the surface charge of the adsorbent and the degree of ionization of adsorbate and particularly on adsorption capacity [1–2,56].

Indeed, it acts both on the surface load of the material by dissociating functional groups on the active sites, and on the forces of the bonds involved in the formation of the molecule-mud complex [6,15].

The pH effect on the adsorption of MB by the sediments is tested at different initial solutions concentrations (100, 500, and 1,000 $mg \cdot L^{-1}$). The study is carried out for pH values between 2 and 12. The pH is adjusted if necessary, at the beginning of the experiment with sodium hydroxide NaOH (Prolabo Normapur) to (0.1 $mol \cdot L^{-1}$) or hydrochloric acid HCl (Prolabo) with concentration (0.1 $mol \cdot L^{-1}$).

As shown in Fig. 6, the amount adsorbed decreases for the three solutions studied with increasing pH up to neutral pH value and then increases, may be related to the preference of dye cations for basic and acidic sites. Results

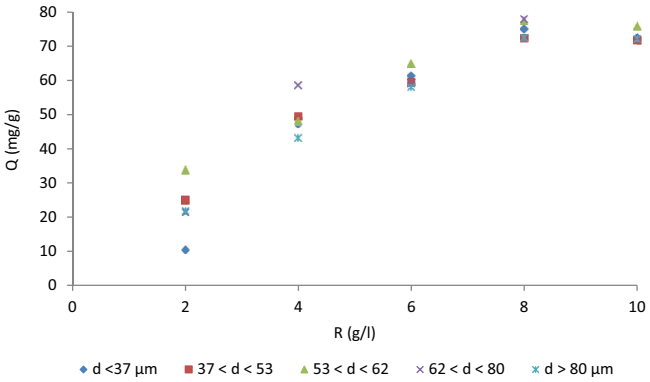

Fig. 5. Effect of the ratio dose on adsorption of methylene blue.

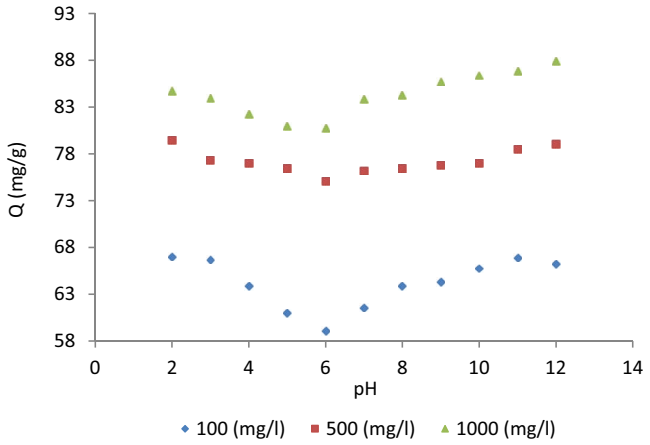

Fig. 6. Variation in the amount of methylene blue adsorbed by the sediment as a function of pH variation for all three solutions.

showed a minimum around pH ~ 6, for the three initial concentrations studied. The dissolution of MB in an acidic medium gives: (A) is the MB dye.

$$ACl + H_2O + HCl \rightarrow A^+ + Cl^- + H_3OCl$$

(A^+) cationic dye.

It is a good hydrogen acceptor. In aqueous media, the cations of the exchangeable dye and those of the surface and region of the intermediate layer of the mud undergo hydration, so we have a hydrophilic environment [57].

Knowing that the mud is a mixture of minerals, formed by the oxides of Al and Si…, these metal oxides form complex hydroxides in solution and the acidic and basic attack of these complexes at the interface solid-solution leads to the development of positive or negative load on the adsorbent surface. In contrast, the acidic medium enhanced the adsorption capacities of methylene blue on the mud samples (Fig. 6). This is presumably due to the adsorption of negative ions (that is, Cl^- from HCl) on the positive surfaces of adsorbent. In a basic medium, the surfaces are negatively charged due to the abundance of OH^- ions on the adsorbent surface, which causes the electrostatic attraction between the dye cations and the negatively charged surface [15]. The

increase in the pH of the adsorbent medium could therefore be responsible for the gradual increase in the adsorption of MB at pH values greater than 6.0. The maximum adsorbed amount of MB is displayed at a pH of about 9 for the three solutions tested [56,58,59]. Some authors find it difficult to explain the increase in adsorption at a pH lower than 4 [26,60].

3.2.3. Effect of the contact time and the initial concentration of the dye

The effect of contact time on the adsorption of the MB on the dam sediment is also studied, for methylene blue solutions of different initial concentrations (100, 500, and 1,000 mg·L^{-1}).

The kinetics of adsorption were studied in flasks of 1,000 mL, where a mass of 5 g of the RMS of the Ghrib dam is mixed with a volume of 500 mL of the MB solution of initial concentrations 100, 500, and 1,000 mg·L^{-1}, at ambient temperature and normal pH of the solution (without correction). Samples for analysis were taken at regular time intervals to determine the final concentrations of the dye. The amount of dye adsorbed at time t, q_t (mg·g^{-1}) was calculated using Eq. (2).

Fig. 7 shows the results of analyses; q_t increases rapidly in the first half-hour for the three solutions and then slows down when the equilibrium is approached [2]. For solutions of initial concentrations (100 mg·L^{-1}), the kinetics are rapid [3,61,62], the equilibrium is achieved after the first 15 min for the other solutions of high concentrations, the equilibrium is reached after 90 min of contact time between adsorbent and adsorbate. Numerous and vacant active surface sites of the adsorbent were available at the initial stage of the reaction, and as time lapsed, the vacant sites reduced in number thereby slowing down the process [62]. Uyar et al. [8] finds a 4 h equilibrium time to fix MB using clay alginate as an adsorbent, the increase in adsorbed amount is negligible after the 100 min of contact time. The increase in the amount of MB adsorbed at equilibrium was found to increase with increase in initial concentration. It ranged from 9.14 mg·g^{-1} for MB solution of initial concentration 100 mg·L^{-1} to 93.72 mg·g^{-1} for MB initial concentration of 1,000 mg·L^{-1} at 20°C and pH = 6. Same results are obtained by Baysal et al. [6] in his study of removal of methylene blue onto Bacillus subtilis, he concluded that the increase of loading capacities is probably due to higher interaction between MB and biosorbent at higher initial concentration. The rate of material transfer is proportional to the concentration gradient and the exchange surface [15]. The experimental data were modeled using the pseudo-first-order and pseudo-second-order (Fig. 8 and Table 2).

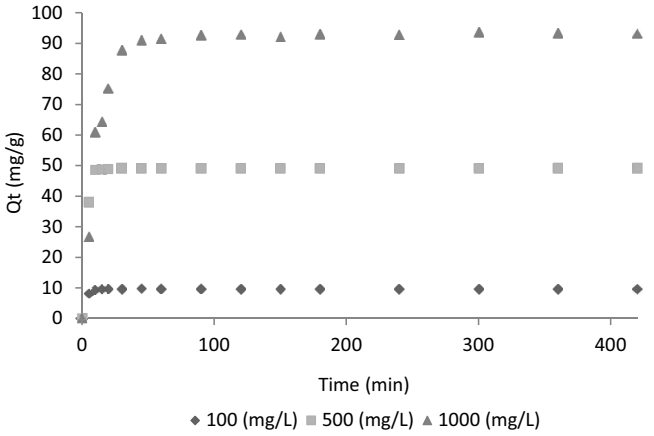

Fig. 7. Effect of contact time on adsorption of methylene blue by raw mud sediment (C_0 = 100, 500 and 1,000 mg·L^{-1}, m = 10 g, V = 1 L, pH = 5.4 and T = 20°C).

3.2.4. Adsorption kinetics

The kinetics and the adsorption mechanism are affected by the physical and chemical characteristics of the adsorbent material [5]. The kinetic study determines the speed of the adsorption process and subsequently calculates the time needed to remove the pollutant [30].

To determine the best kinetic model corresponding to the experimental adsorption data, the pseudo-first-order model was used (pseudo-first-order).

It was assumed in this model that the rate of adsorption at the instant t is proportional to the difference between the amount adsorbed Q_e at equilibrium and the amount q_t adsorbed at that time, and that adsorption is reversible [27].

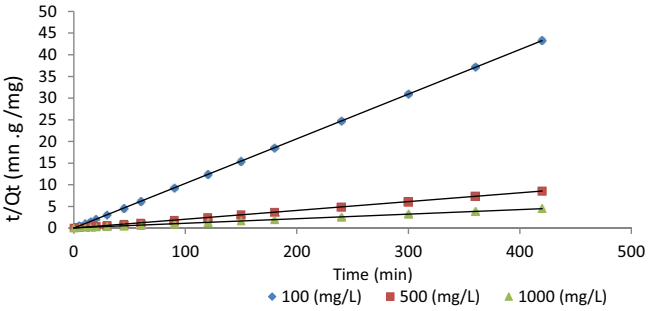

Fig. 8. Modeling of the adsorption kinetics according to the pseudo-second-order kinetic model for initial concentrations (100, 500, and 1,000 mg·L^{-1}).

Table 2
Kinetic parameters of the adsorption of methylene blue on the crude mud according to the initial concentration

Adsorbent	Parameters	Raw mud sediment		
		C_i (mg·L^{-1})		
		100	500	1,000
Kinetic models	Q_e exp (mg·g^{-1})	9.81	49.23	93.72
First-order	K_1 10^3 (min^{-1})	4.84	9.21	10.82
kinetic model	Q_e (mg·g^{-1})	0.400	1.033	13.84
	R^2	0.23	0.4	0.62
Second-order	K_2 (g·mg^{-1}·min^{-1})	1.14	7.9 × 10^{-2}	2.58 × 10^{-3}
kinetic model	Q_e (mg·g^{-1})	9.708	49.26	94.34
	R^2	1.0	1.0	0.99
Intraparticle	K_p (mg·g^{-1}·min^{-1})	0.0024	0.014	0.144
diffusion	C (mg·g^{-1})	9.74	48.92	90.74

The rate law is written:

$$\frac{dq_t}{dt} = K_1\left(Q_e - q_t\right) \tag{3}$$

After integrating Eq. (3) between moments 0 and t (min):

$$\log\left(q_e - q_t\right) = \log q_e - \frac{K_1}{2.303}t \tag{4}$$

where K_1: is the rate constant of adsorption that has the inverse dimension of time (min^{-1}); q_e and q_t ($mg{\cdot}g^{-1}$) are the amounts of dye adsorbed on the material adsorbents at the equilibrium and at instant t, respectively.

In the case of apparent pseudo-first-order kinetics, the plot of $\log(q_e - q_t)$ as a function of time gives a slope line $K_1/2{,}303$ and y-intercept $\log q_e$.

The kinetics of the pollutant fixation reaction on the adsorbent is ugly successfully described by the pseudo-second-order. The pseudo-second-order adsorption kinetic rate equation is expressed in Eq. (5):

$$\frac{dq}{dt} = K_2\left(Q_e - q_t\right)^2 \tag{5}$$

The integration of Eq. (5) followed by its linearization gives us.

$$\frac{t}{q_t} = \frac{1}{K_2 Q_e^2} + \frac{1}{Q_e}\cdot t \tag{6}$$

where Q_e and q_t ($mg{\cdot}g^{-1}$) adsorption capacity of the sediments at saturation and at the moment t, respectively; K_2 ($g{\cdot}mg^{-1}{\cdot}min^{-1}$) is the pseudo-second-order rate constant.

The path of t/q_t according to time (t) will give a right slope $1/Q_e$ and order originally $1/K_2Q_e^2$.

These values allow the determination of the apparent rate constant K_2 and the adsorption capacity of the material at saturation (Q_e).

The results obtained by applying the pseudo-first-order are shown in Table 2. The respective values of the correlation coefficients R^2 (0.23, 0.4, and 0.62) for MB solutions of initial concentrations (100, 500, and 1,000 $mg{\cdot}L^{-1}$) are low. They do not match the path of a straight line. This leads us to conclude that the pseudo-first-order does not apply to the three studied solutions [15,63]. The large difference between the experimental Q_e ($mg{\cdot}g^{-1}$) and Q_e(cal) ($mg{\cdot}g^{-1}$) values calculated according to Lagergren reinforces the cited remarks.

The plot of t/q_t as a function of time (t) [Eq. (6)] gives straight lines (Fig. 8). The R^2 values listed for pseudo-second-order model were between 0,999 and 1 (Table 2), which are higher than the obtained R^2 values for the pseudo-first-order model. It is noteworthy that all kinetic data were best described by the pseudo-second-order kinetic model irrespective of the different initial concentration in MB onto RMS adsorbent [1]. There was also a better agreement between experimental Q_e and calculated Q_e(cal), for the three solutions with a difference from – 0.66% to 1.05%. This suggests that the adsorption process involves the transport of solute molecules from the aqueous solution to the surface of solid particles followed by intraparticle diffusion, as observed by some previous works [6,7].

3.2.5. Intragranular diffusion model

During adsorption, there is a series of resistances to mass transfer (external or internal resistances). Also, it is known that adsorption process is governed by diffusion in the liquid film (external diffusion) and the diffusion in adsorbent particle (internal diffusion). So, in order to obtain information about the diffusion mechanism, the kinetic results were analyzed by the intragranular diffusion model expressed by the Webber–Morris equation [49,64].

$$q_t = K_p \cdot t^{1/2} + C \tag{7}$$

where q_t: quantity of methylene blue fixed per unit mass of adsorbent material ($mg{\cdot}g^{-1}$) at instant t; K_p: intraparticle diffusion rate parameter ($mg{\cdot}g^{-1}{\cdot}min^{-1}$) and values of intercept C gives an idea about the thickness of boundary layer. This is attributed to the instantaneous utilization of the most readily available adsorbing sites on the adsorbent surface ($mg{\cdot}g^{-1}$) [64].

The plot of $t^{1/2}$ vs. q_t [Eq. (7)] is presented in Fig. 9. The results of intraparticle diffusion have shown that all curves in this figure have two branches; one inclined corresponding to a bulk adsorption stage of an increasing amount of dye and the other of a low slope corresponding to the establishment of a balance. The curves do not pass through the origin, suggesting that diffusion is not the only rate-limiting step in the adsorption process. The first linear region corresponds to the diffusion through a boundary layer (mesopores and macropores). The second region is the gradual adsorption stage, which is attributed to the diffusion from mesopores and macropores to micropores [65]. Diffusion in the pores can have a considerable influence on the kinetics of adsorption, but it is not the only factor controlling the rate of the kinetics [21,64]. The surface and other processes such as interparticle diffusion can contribute to the diffusion process [66].

3.2.6. Adsorption isotherms

Adsorption isotherms are often used for the determination of maximum pollutant fixation capacities and the identification of the type of adsorption [15,67].

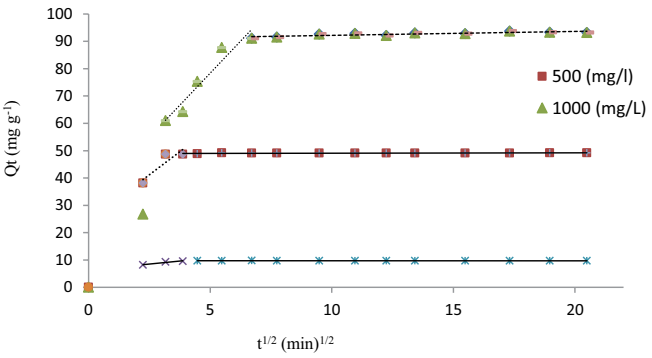

Fig. 9. Intraparticle diffusion model for adsorption of methylene blue onto the mud sediment.

We have tried to characterize the experimental results of the adsorption of MB on the RMS of the Ghrib dam (from Algeria) according to the mathematical models of Langmuir, Freundlich and Temkin models.

3.2.6.1. Langmuir model

The Langmuir isotherm is based on the assumption that adsorption takes place on homogeneous sites within the adsorbent. There was no significant interaction between the adsorbed species. The adsorbent is saturated after the formation of a layer of adsorbate on its surface [68].

To obtain these two equilibrium parameters of the Langmuir model, the linearization version can be envisaged, in the form:

$$\frac{C_e}{Q_e} = \frac{1}{K_L \cdot Q_{\max}} + \frac{C_e}{Q_{\max}} \tag{8}$$

Another R_L equilibrium parameter (Hall parameter) can be determined using the isothermal characteristics of Langmuir, it is calculated as:

$$R_L = \frac{1}{1 + K_L \cdot C_0} \tag{9}$$

where C_0: initial concentration (mg·L^{-1}), K_L: Langmuir constant (L·mg^{-1}).

If $R_L > 1$, adsorption is unfavorable, ($R_L = 1$) Indicates the adsorption is linear, when ($0 < R_L < 1$) adsorption is favorable and if ($R_L = 0$) adsorption is irreversible [2,15,69].

3.2.6.2. Freundlich model

The Freundlich isotherm, one of the most used empirical equations, describes the non-ideal adsorption. The model assumes a heterogeneous surface with a non-uniform distribution of heat of adsorption over the surface [1,22]. The model can be expressed by Eq. (10):

$$Q_e = K_F C_e^{1/n} \tag{10}$$

where Q_e: quantity of dye adsorbed by the mass m of adsorbent (mg·g^{-1}); K_F, n: constants for a given adsorbent and solute dependent on temperature, related, respectively to the adsorption capacity and intensity. 1/n: is a parameter related to the surface heterogeneity or nature of adsorption [8,65]; C_e: solute concentration at the adsorption equilibrium (mg·L^{-1}).

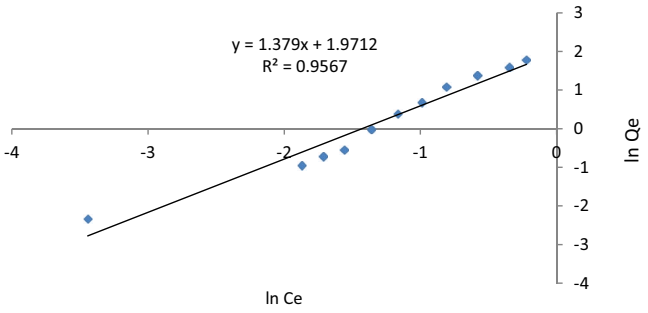

Fig. 10. Modeling of adsorption results following the Freundlich isotherm model.

The linearization of Eq. (10) gives:

$$\log Q_e = \log K_F + \frac{1}{n} \cdot \log C_e \tag{11}$$

By tracing $\log Q_e = f(\log C_e)$, we can determine the values of the constants K_F and n of Freundlich isotherm.

Fig. 10 represents the results of the model, and Table 3 presents the different parameters of the three models used.

3.2.6.3. Temkin model

The Temkin adsorption isotherm model based on the heat of pollutant adsorption, and the adsorption is characterized by a uniform distribution of the binding energies, up to some maximum binding energy [62], this model is done by Eq. (12). The Temkin equation suggests a linear decrease of sorption energy as the degree of completion of the sorptional centers of an adsorbent is increased.

$$Q_e = \frac{RT}{b_T} \ln K_T + \frac{RT}{b_T} \ln C_e \tag{12}$$

where T: absolute temperature in (°K), b_T the isotherm Temkin constant (J·mol^{-1}), K_T the equilibrium binding constant corresponding to the maximum binding energy.

Fig. 11 represents the results of the modeling. The results show that the retention capacity of the experimentally evaluated sediments is close to that calculated theoretically (Table 3). The adsorption isotherms (Fig. 11) shows that the adsorption is better characterized by the Langmuir model for solutions of MB at higher initial concentrations (>100 mg·L^{-1}) (R^2 = 0.9919) than for the MB solutions at low initial concentrations (<100 mg·L^{-1}), which leads to the absence of interaction between the adsorbed pollutants. The calculated value of R_L using the expression [Eq. (9)] is in all

Table 3
Adsorption equilibrium parameters according to the Langmuir, Freundlich and Temkin models

Adsorbent	Raw mud sediment	
Isothermal models	Parameters	Values
Langmuir model	$Q_{\max}$ (exp.) (mg·g^{-1})	104.66
	K_L (L·mg^{-1})	0.019
	R^2	0.9958
	$Q_{\max}$ (cal.) (mg·g^{-1})	109.89
	R_L	0.05
Freundlich model	1/n	0.4691
	K_F	5.98
	R^2	0.7594
Temkin model	K_T (L·mg^{-1})	1.81
	b_T (J·mol^{-1})	200.61
	R^2	0.66

cases between 0 and 1, which means that the adsorption is favorable (Fig. 12) [15,69,70].

The results presented in Fig. 10 show that the Freundlich model is better suited for solutions with low initial concentrations [26], than for solutions with high initial concentrations. The value of $1/n$ is less than 1, which suggests that the adsorption sites are heterogeneous. It is generally stated that for values of $n < 1$, adsorption is low. If the values of n are between $0 < n < 1$, adsorption is moderately difficult [8,66–68], the values of the Freundlich constant n are greater than unit, suggesting a favorable adsorption process [64].

Low R^2 value is observed in the case of Temkin model; indicate that adsorption is not described by this isotherm model. The value of b_T is 0.2 kJ·mol^{-1} indicating a low interaction between the adsorbent and adsorbate [67].

For the curves obtained for nonlinear shapes, and especially for low concentrations, it is observed that more than one model can be valid to express the mode of retention.

The plot logQ_e based on logC_e for the MB studied solutions is shown in Fig. 10. The results show (Table 3) that the Freundlich model is better suited for solutions with low initial concentrations ($R^2 = 0.95$ and $0 < n < 1$) [26], than for solutions with high initial concentrations ($R^2 = 0.76$ and $n > 1$). It is generally stated that for values of $n < 1$, adsorption is low. If the values of n are between $0 < n < 1$, adsorption is moderately difficult, on the other hand, n values above the unity indicate that adsorption is a favorable physical process [1,69–71]. The equilibrium value of $n = 2.13$ (Table 3) suggests favorable adsorption and that physical adsorption is dominant.

The correlation coefficients calculated from Temkin isotherm equation (Table 3) reveals that the dye adsorption at 298 K is characterized by a uniform distribution of binding energies up to some maximum binding energy. The increasing temperature probably leads to a decrease of uniformity.

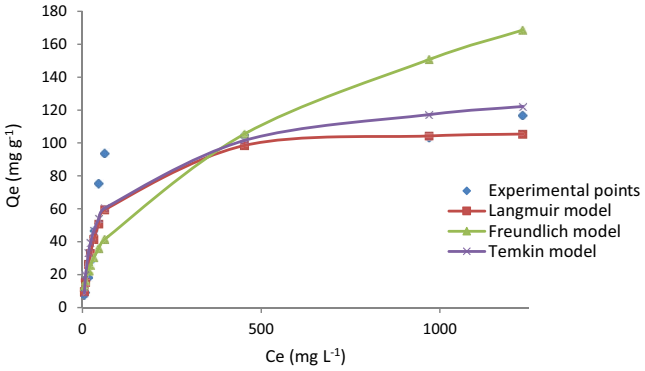

Fig. 11. Adsorption isotherms of methylene blue on raw sediments of the dam.

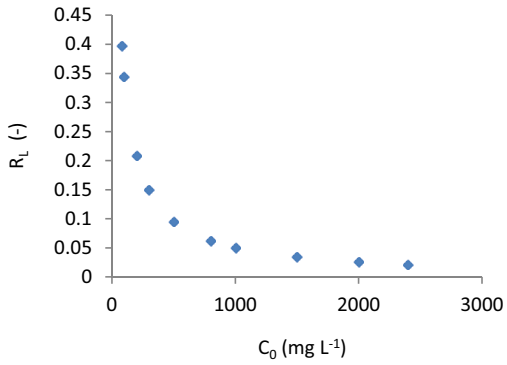

Fig. 12. Variation of R_L as a function of methylene blue initials concentrations solutions onto raw mud sediment.

3.2.7. Comparison of adsorption capacity of different adsorbents

The comparison of maximum adsorption capacity (Q_{max}) of methylene blue onto various adsorbents are listed in Table 4. The (Q_{max}) values reported in Table 4 were obtained using the best experimental conditions of each study. The adsorbent studied in this work, displayed the best adsorption capacity among the different sorbents. It exhibited that adsorbent in this study could certainly be competitive with other adsorbents and it could be used as a promising adsorbing material in the wastewater treatment, given an indication that this adsorbent is very efficient.

3.2.8. Thermodynamic parameters

Thermodynamic parameters for the adsorption process such as the standard enthalpy $\Delta H°$ (kJ·mol^{-1}), the standard entropy $\Delta S°$ (kJ·mol^{-1}·K^{-1}) and the standard free enthalpy $\Delta G°$ (kJ·mol^{-1}) can be evaluated using the Eqs. (13)–(15) [72,73]:

$$K_d = \frac{Q_e}{C_e} \tag{13}$$

$$\Delta G° = -R \cdot T \cdot \ln K_d \tag{14}$$

$$\Delta G° = \Delta H° - T \cdot \Delta S° \tag{15}$$

Eqs. (14) and (15) may be expressed as:

$$\ln K_d = \frac{\Delta S°}{R} - \frac{\Delta H°}{R}\frac{1}{T} \tag{16}$$

Table 4
Maximum adsorption capacity Q_m (mg·g^{-1}) of methylene blue by various adsorbents in other reports

Adsorbents	Q_m (mg·g^{-1})	References
Crude dam mud (Algeria)	104.66	This work
Activated lignin-chitosan	36.3	[72]
Fe_3O_4/Mt	106.4	[73]
Kaolin	45.0	[74]
Raw KT3B kaolin (Algeria)	52.76 (25°C)	[15]
Raw coal-bearing kaolin	78.1	[75]

Table 5
Thermodynamic parameters of the adsorption of methylene blue on sediments

Temperature (°C)	Temperature (°K)	1,000·1/T (°K^{-1})	$\Delta H°$ (kJ·mol^{-1})	$\Delta S°$ (J·mol^{-1}·K^{-1})	$\Delta G°$ (kJ·mol^{-1})
20	293.15	3.41	–19.60	–35.32	–9.28
30	303.15	3.29			–8.86
40	313.15	3.19			–8.53
50	323.15	3.09			–8.19

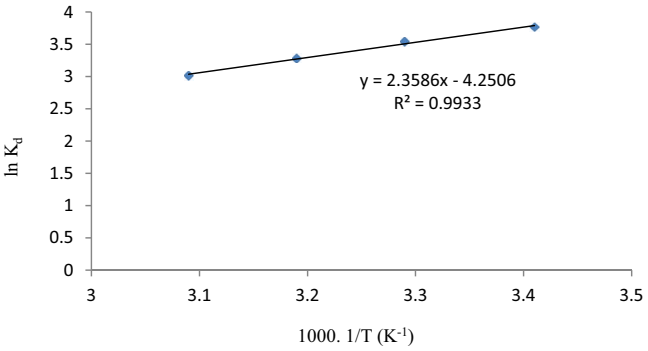

Fig. 13. Effect of temperature on the distribution constant of the adsorption phenomenon of methylene blue on the raw mud sediment (lnK_d) as a function of (1/T).

We have renewed the same adsorption process that we have followed in the case of other tests. The initial concentration C_0 = 100 mg·L^{-1} of the MB solution was selected. To test the influence of temperature on the phenomenon of adsorption by the raw mud, the temperature of the adsorption medium was varied between 20°C and 50°C.

The evolution of lnK_d as a function of 1/T (Fig. 13) allowed us to deduce the thermodynamic parameters related to the adsorption of MB on the RMS. It shows an increase in the lnK_d when the inverse of the temperature (1/T) increases. Table 5 gives the results of thermodynamic study, in this temperature range, the structure of the mud is not affected and so is the stability of the dye. The values of the three parameters $\Delta H°$, $\Delta S°$ and $\Delta G°$ of the system demonstrate a spontaneous, favorable, and exothermic process [15,74].

The negative value of apparent enthalpy change $\Delta H°$ highlights the possibility of an exothermic process of dye adsorption. The values of the activation energy are ≤40 (kJ·mol^{-1}) indicate that the adsorption of MB on the RMS is physical, involving weak interactions between reactive dye molecules and the charged groups onto adsorbent surface [6,27,64]. The standard entropy change value ($\Delta S°$) is not very large and the negative value indicates decreased disorder at the solid–liquid interface during dye sorption. As the temperature is increased, the mobility of dye ions increases causing the ions to form an active complex controlled by an associated mechanism [5,56].

The negative values of the Gibbs free energy change ($\Delta G°$) (Table 5) as a function of the increase temperature T (°K) are indicative of the spontaneous nature of the interaction without requiring large energies of adsorption activation [8,27,75]. It is also noted that ($\Delta G°$) increases with the increase of the temperature of the solution, which can be explained by the fact that adsorption becomes very difficult and disadvantaged when the temperature becomes very large [27]. The adsorption of MB is rapid and more spontaneous at low temperatures [22].

4. Conclusion

The present study allows us to conclude that the adsorption of MB by muddy sediment is possible. The adsorption studies were carried out as a function of contact time, initial dye concentration, solution pH, and temperature. The percentage removal of the dye molecule increased with increase in initial dye concentration, and contact time.

Batch studies demonstrated that under laboratory conditions, a 10 g·L^{-1} adsorbent dose was found to be optimum at a pH of 5.6, contact time of 120 min and temperature of 25°C for achieving a removal rate greater than 52% of MB ions from synthetic solution, containing 1,000 mg·L^{-1} of MB ions concentration. The kinetic study shows that the adsorption equilibrium is rapidly reached for dye solutions at low concentration (15 min), it is 120 min for solutions of more than 1,000 mg·L^{-1} of initial concentrations.

The adsorption kinetics is very well controlled by pseudo-second-order regardless of the initial concentration of the dye solution. Indeed, the adsorbed amounts are better at pH < 5 and pH > 7. It records a low fixation rate at a pH around 6.

Equilibrium adsorption was achieved in about 120 min. The equilibrium adsorption data analyzed by the Langmuir, Freundlich, and Temkin isotherm models revealed that the isotherm of the solution with initial concentration C_0 < 100 mg·L^{-1} obeys the Freundlich isotherm, and those of concentrations greater than 100 mg·L^{-1} follows the Langmuir model (R^2 = 0.9919), indicating monolayer sorption on a homogenous surface. The monolayer sorption capacity was 93.72 mg·g^{-1} for an initial concentration of 1,000 mg·L^{-1}, which was achieved at a temperature of 293 K and pH of 5.6. Adsorption of MB on dam sediment sample seems to be a favored process. The value of Freundlich constant n = 2.13 suggests favorable adsorption with physical adsorption dominance.

The correlation coefficients calculated from Temkin isotherm equation (Table 3) reveals that the dye adsorption at 298 K is characterized by a uniform distribution of binding energies up to some maximum binding energy. The increasing temperature probably leads to a decrease of uniformity.

Thermodynamic parameters such as change in Gibbs free energy $\Delta G°$, adsorption enthalpy ($\Delta H°$), and adsorption entropy ($\Delta S°$) were also estimated. The enthalpy change

value ($\Delta H°$ = –19.6 kJ·mol^{-1}) suggests that the adsorption process is exothermic. The negative sign of $\Delta S°$ = –35.32 J·mol^{-1}·K^{-1} indicates that the adsorption process is done by electrostatic interaction between the adsorbent surface and the adsorbate species in solution. The negative values of $\Delta G°$ show that the adsorption process is spontaneous. The values of the activation energy are ≤40 (kJ·mol^{-1}) indicate that the adsorption of MB on the crude mud is physical.

According to the present findings, muddy sediments can be a promising adsorbent for cationic dyes removal from aqueous solution.

Acknowledgments

The authors would like to thank the Ministry of Higher Education and Scientific Research in Algeria (MHESR) for offering the scholarship for realization of this work. As they also thank the members of the chemical engineering laboratory for their collaboration in this study.

References

[1] E.E. Özbas, A. Öngen, C.E. Gökçe, Removal of Astrazon Red 6B from aqueous solution using waste tea and spent tea bag, Desal. Water Treat., 51 (2013) 7523–7535.
[2] D.S. Tong, C.W. Wu, M.O. Adebajo, G.C. Jin, W.H. Yu, S.F. Ji, C.H. Zhou, Adsorption of methylene blue from aqueous solution onto porous cellulose-derived carbon/montmorillonite nanocomposites, Appl. Clay Sci., 161 (2018) 256–264.
[3] F.P. de Sá, B.N. Cunha, L.M. Nunes, Effect of pH on the adsorption of Sunset Yellow FCF food dye into a layered double hydroxide (CaAl-LDH-NO_3), Chem. Eng. J., 215–216 (2013) 122–127.
[4] I. Savic, D. Gajic, S. Stojiljkovic, I. Savic, S. di Gennaro, Modeling and Optimization of Methylene Blue, Adsorption from Aqueous Solution Using Bentonite Clay, Proceedings of the 24 European Symposium on Computer Aided Process Engineering – ESCAPE, Budapest, Hungary, 2014, pp. 15–18.
[5] K. Rida, S. Bouraoui, S. Hadnine, Adsorption of methylene blue from aqueous solution by kaolin and zeolite, Appl. Clay Sci., 83–84 (2013) 99–105.
[6] A. Ayla, A. Çavuş, Y. Bulut, Z. Baysal, Ç. Aytekin, Removal of methylene blue from aqueous solutions onto *Bacillus subtilis*: determination of kinetic and equilibrium parameters, Desal. Water Treat., 51 (2013) 7596–7603.
[7] J. Zhang, Q. Ping, M. Niu, H. Shi, N. Li, Kinetics and equilibrium studies from the methylene blue adsorption on diatomite treated with sodium hydroxide, Appl. Clay Sci., 83–84 (2013) 12–16.
[8] G. Uyar, H. Kaygusuz. F.B. Erim, Methylene blue removal by alginate–clay quasi-cryogel beads, React. Funct. Polym., 106 (2016) 1–7.
[9] G. Rytwo, Applying a Gouy–Chapman–Stern model for adsorption of organic cations to soils, Appl. Clay Sci., 24 (2004) 137–147.
[10] Y. Xu, B. Sun, Y. Cao, C. Chen, Recyclable green hydrogel adsorbents with excellent adsorption capacity for removal of methylene blue, Desal. Water Treat., 291 (2023) 170–181.
[11] B. de Souza, G. Proença, R. de Souza Antonio, L.F. Cusioli, M.F. Vieira, R. Bergamasco, A. Marquetotti, S. Vieira, Assessment of the natural zeolite adsorption capacity for the removal of triclosan from the aqueous medium, Desal. Water Treat., 292 (2023) 165–175.
[12] N. Tom, O. Brine, Wastewater pretreatment using clay minerals and organoclays as flocculants, Appl. Clay Sci., 67–68 (2012) 119–124.
[13] S. Bentahar, A. Dbik, M. El Khomri, N. El Messaoudi, A. Lacherai, Adsorption of methylene blue, crystal violet, and Congo red from binary and ternary systems with natural clay: kinetic, isotherm, and thermodynamic, J. Environ. Chem. Eng., 5 (2017) 5921–5932.
[14] A.M. Mosaku, A.K. Akinlabi, O.S. Sojinu, M.K.O. Arifalo, A.A. Falomo, G. Oladipo, S. Oni, F.Y. Falope, N.Y. Ilesanmi, V.N. Diayi, Adsorptive remediation of oil spill contaminated water using chitosan modified natural rubber as adsorbent, Chem. Afr., 4 (2021) 535–543.
[15] A.T. Khan, S. Dahiya, I. Ali, Use of kaolinite as adsorbent: equilibrium, dynamics, and thermodynamic studies on the adsorption of Rhodamine B from aqueous solution, Appl. Clay Sci., 69 (2012) 58–66.
[16] V. Vimonses, S. Lei, B. Jin, W. Chris, K. Chow, C. Saint, Adsorption of Congo red by three Australian kaolins, Appl. Clay Sci., 43 (2009) 465–472.
[17] I. Dékány, L. Turi, A.F. János, B. Nagy, The structure of acid-treated sepiolites: small-angle X-ray scattering and multi MAS-NMR investigations, Appl. Clay Sci., 14 (1999) 141–160.
[18] L. Mouni, L. Belkhiri, J.C. Bollinger, A. Bouzaza, A. Assadi, A. Tirri, F. Dahmoune, K. Madani, H. Remini, Removal of methylene blue from aqueous solutions by adsorption on kaolin: kinetic and equilibrium studies, Appl. Clay Sci., 153 (2018) 38–45.
[19] S.W. Nahm, W.G. Shim, Y.K. Park, S.C. Kim, Thermal and chemical regeneration of spent activated carbon and its adsorption property for toluene, Chem. Eng. J., 210 (2012) 500–509.
[20] A. Chahi, F. Weber, L. Prevot, J. Lucas, The use of cation exchange resins (Amberlite IRC-50H) in the dispersion and purification of clays of carbonates, phosphates, and sulphates, Clay Miner., 28 (1993) 585–601.
[21] G.L. Dotto, J.M. Moura, T.R.S. Cadaval, L.A.A. Pinto, Application of chitosan films for the removal of food dyes from aqueous solutions by adsorption, Chem. Eng. J., 214 (2013) 8–16.
[22] J. Deng, M. Liu, X. Gong, H. Tao, *Ipomoea batatas* vine-derived activated carbon: a utility and efficient adsorbent for removing Cr(VI) from aqueous solution, Desal. Water Treat., 292 (2023) 108–121.
[23] G. Suraj, C.S.P. Iyer, M. Lalithambika, Adsorption of cadmium and copper by modified kaolinites, Appl. Clay Sci., 13 (1998) 293–306.
[24] S. El Harfaoui, Z. Zmirli, A. Mohssine, A. Driouich, B. Sallek, K. Digua, H. Chaair, Model development for the treatment of toxic industrial wastewaters by a coagulation process: an easy tool for linking experimental and theoretical data, Desal. Water Treat., 291 (2023) 72–91.
[25] B. Doušová, M. Lhotka, T. Grygar, V. Machovič, L. Herzogová, *In-situ* co-adsorption of arsenic and iron/manganese ions on raw clays, Appl. Clay Sci., 54 (2011) 166–171.
[26] Y. Weldemariam, D. Enke, D. Schneider, Thermochemical purification, technical properties, and characterization of Ethiopian diatomite from Adami-Tulu deposit, Chem. Afr., 2 (2019) 733–740.
[27] A. Aarfane, A. Salhi, M. El Krati, S. Tahiri, M. Monkade, Kinetic and thermodynamic study of the adsorption of Red195 and methylene blue dyes on fly ash and bottom ash in aqueous medium, J. Mater. Environ. Sci., 5 (2014) 1927–1939.
[28] R. Chitrakar, Y. Makita, A. Sonoda, T. Hirotsu, Adsorption of trace levels of bromate from aqueous solution by organo-montmorillonite, Appl. Clay Sci., 51 (2011) 375–379.
[29] T. Kan, X. Jiang, L. Zhou, M. Yang, M. Duan, P. Liu, X. Jiang, Removal of methyl orange from aqueous solutions using a bentonite modified with a new Gemini surfactant, Appl. Clay Sci., 54 (2011) 184–187.
[30] M. Bagane, S. Guiza, Removal of a dye from textile effluents by adsorption, Ann. Chim. Sci. Mat., 25 (2000) 615–625.
[31] Z. Dali-Youcef, H. Bouabdasselem, N. Bettahar, Elimination of organic compounds by local clays, C.R. Chim., 9 (2006) 1295–1300.
[32] B. Remini, Valorization of the silt of the dams some Algerian examples, Larhyss J., 5 (2006) 75–89.
[33] B. Remini, D. Bensafia, Siltation of dams in arid regions Algerian examples, Larhyss J., 27 (2016) 63–90.

[34] K. Ouhba, L. Benamara, A. Hadj Hamoui, A. Hamwi, A. Marie, D. Loye Pilot, Conception of a synthesis pozzolan from sediment dams calcined (Case: Gargar dams), MATEC Web Conf., 11 (2014) 01023, doi: 10.1051/matecconf/20141101023.
[35] N. Bouhamou, A. Mebrouki, N. Belas, S. Aggoun, A. Benaissa, A. Kheirbek, Valorization of Natural Waste in the development of New Concretes and Construction Materials, 20th French Congress of Mechanics, August 29 to September 2, Besançon, 2011.
[36] G. Aubert, Soil Analysis Methods. National Pedagogic Documentation Center, Printing service 55 rue Sylvabelle 13006 Marseille.
[37] Y. Yukselen, A. Kaya, Suitability of the methylene blue test for surface area, cation exchange capacity, and swell potential determination of clayey soils, Eng. Geol., 102 (2008) 38–45.
[38] J.C. Santamarina, K.A. Klein, Y.H. Wang, E. Prencke, Specific surface: determination and relevance, Can. Geotech. J., 39 (2002) 233–241.
[39] Y. Yukselen, A. Kaya, Comparison of methods for determining specific surface area of soils, J. Geotech. Geoenviron. Eng., 132 (2006) 931–936.
[40] A. Amari, M. Chlendi, A. Gannouni, A. Bellagi, Optimized activation of bentonite for toluene adsorption, Appl. Clay Sci., 47 (2010) 457–461.
[41] M. Suàrez, E. Garcia Romero, Variability of the surface properties of sepiolite, Appl. Clay Sci., 67–68 (2012) 72–82.
[42] M. Hajjaji, S. Kacim, M. Boulmane, Mineralogy and firing characteristics of a clay from the valley of Ourika (Morocco), Appl. Clay Sci., 21 (2002) 203–212.
[43] D. Benyerou, N. Boudjenane, M. Belhadri, Comparative Study on the Physicochemical Characteristics of Harbor Dredging Sediments and Slip Used in the Manufacture of Bricks, Symposium 01 Ecomaterials, 2014.
[44] J.T. Kloprogge, R. Evans, L. Hickey, R.L. Frost, Characterization and Al-pillaring of smectites from Miles, Queensland (Australia), Appl. Clay Sci., 20 (2002) 157–163.
[45] M.S. Hassan, N.A. Abdel-Khalek, Beneficiation, and applications of an Egyptian bentonite, Appl. Clay Sci., 13 (1998) 99–115.
[46] Q. Wu, Z. Li, H. Hong, Adsorption of the quinoloneantibiotic nalidixic acid onto montmorillonite and kaolinite, Appl. Clay Sci., 74 (2013) 66–73.
[47] M. Abrougui, M.D. Bahri, E. Srasra, Structural characterizations and viscosity behavior of purified clay obtained by hydrocyclone process, Chem. Afr., 2 (2019) 741–747.
[48] M. Felhi, A. Tlili, M.E. Gaied, M. Montacer, Mineralogical study of kaolinitic clays from Sidi El Bader in the far north of Tunisia, Appl. Clay Sci., 39 (2008) 208–217.
[49] Y.L. Cao, Z.H. Pan, Q.X. Shi, J.Y. Yu, Modification of chitin with high adsorption capacity for methylene blue removal, Int. J. Biol. Macromol., 114 (2018) 392–399.
[50] P. Ranjan, S.C. Datta, K.M. Manjaiah, R. Bhattacharyya, X-ray crystallinity of different soil nanoclays in relation to phosphatase adsorption, Appl. Clay Sci., 144 (2017) 19–25.
[51] P.T. Hang, G.W. Brindley, Methylene blue absorption by clay minerals, determination of surface areas and cations exchange capacities (clay-organic studies XVIII), Clays Clay Miner., 18 (1970) 203–212.
[52] G. Kahr, F.T. Madsen, Determination of the cation exchange capacity and the surface area of bentonite, illite, and kaolinite by methylene blue adsorption, Appl. Clay Sci., 9 (1995) 327–336.
[53] J.M. Konrad, F. Alonso, V. Gabezas, Characterization of Fine Particles of a Granular Foundation Material by the Methylene Blue Test, Report GCT-2008-01, CREIG.
[54] A. Lecloux, Exploitation of Nitrogen Adsorption and Desorption Isotherms for the Study of the Texture of Porous Solids, Brief of the Royal Society of Sciences of Liège, 6th Series, T1 Fascicule 4, 1971, pp. 169–209.
[55] L. Meier, P.K. Guenter, Determination of the cation exchange capacity (CEC) of clay minerals using the complexes of copper(II) ion with triethylenetetramine and tetraethylenepentamine, Clays Clay Miner., 47 (1999) 386–388.
[56] S. Karaca, A. Gürses, Ö. Açışlı, A. Hassani, M. Kıranşan, K. Yıkılmaz, modeling of adsorption isotherms and kinetics of Remazol Red RB adsorption from aqueous solution by modified clay, Desal. Water Treat., 51 (2013) 2726–2739.
[57] T.A.H. Nguyen, H.H. Ngo, W.S. Guo, J. Zhang, S. Liang, K.L. Tung, Feasibility of iron-loaded 'Okara' for biosorption of phosphorous in aqueous solutions, Bioresour. Technol., 150 (2013) 42–49.
[58] R. Zhu, Q. Chen, Q. Zhou, Y. Xi, J. Zhu, H. He, Adsorbents based on montmorillonite for contaminant removal from water: a review, Appl. Clay Sci., 123 (2016) 239–258.
[59] M. Hajjaji, A. Alami, Influence of operating conditions on methylene blue uptake by a smectite rich clay fraction, Appl. Clay Sci., 44 (2009) 127–129.
[60] A.B. Albadarin, M.N. Collins, M. Naushad, S. Chirazian, G. Walker, C.M. Gwandi, Activated lignin-chitosan extruded blends for efficient adsorption of methylene blue, Chem. Eng. J., 307 (2017) 264–272.
[61] J. Bujdák, M. Janek, J. Madejová, P. Komadel, Methylene blue interactions with reduced-charge smectites, Clays Clay Miner., 49 (2001) 244–254.
[62] A.M. Monique Lawrence, R.K Kukkadapu, S.A. Boyd, Adsorption of phenol and chlorinated phenols from aqueous solution by tetramethylammonium - and tetramethylphosphonium - exchanged montmorillonite, Appl. Clay Sci., 13 (1998) 13–20.
[63] S. Gammoudi, N. Frini-Srasra, E. Srasra, Influence of exchangeable cation of smectite on HDTMA adsorption: equilibrium, kinetic and thermodynamic studies, Appl. Clay Sci., 69 (2012) 99–107.
[64] M.N. Zeid, A. ALOthman, Md.R. Awual, S.M. Alfadul, T. Ahamad, Adsorption of rose Bengal dye from aqueous solution by Amberlite Ira-938 resin: kinetics, isotherms, and thermodynamic studies, Desal. Water Treat., 57 (2016) 13527–13533.
[65] I. Othman, M.A. Haija, P. Kannan, Adsorptive removal of methylene blue from water using high-performance alginate-based beads, Water Air Soil Pollut., (2020) 231–396.
[66] K.M. Seliem, S. Komarneni, T. Byrne, F.S. Cannon, M.G. Shahien, A.A. Khalil, I.M.A. El-Gaid, Removal of perchlorate by synthetic organosilicas and organoclay: kinetics and isotherm studies, Appl. Clay Sci., 71 (2013) 21–26.
[67] M. Auta, B.H. Hameed, Modified mesoporous clay adsorbent for adsorption isotherm and kinetics of methylene blue, Chem. Eng. J., 198–199 (2012) 219–227.
[68] A.S. Ibupoto, U.A. Qureshi, F. Ahmed, Z. Khatri, M. Khatri, M. Maqsood, R.Z. Brohi, I.S. Kim, Reusable carbon nanofibers for efficient removal of methylene blue from aqueous solution, Chem. Eng. Res. Des., 136 (2018) 744–752.
[69] Ö. Şahina, M. Kayaa, Cafer Saka, Plasma-surface modification on bentonite clay to improve the performance of adsorption of methylene blue, Appl. Clay Sci., 116–117 (2015) 46–53.
[70] Y. Miyah, M. Idrissi, F. Zerrouq, Study and modeling of the kinetics methylene blue adsorption on the clay adsorbents (pyrophillite, calcite), J. Mater. Environ. Sci., 6 (2015) 699–712.
[71] D. Xu, X.L. Tan, C.L. Chen, X.K. Wang, Adsorption of Pb(II) from aqueous solution to MX-80 bentonite: effect of pH, ionic strength, foreign ions and temperature, Appl. Clay Sci., 41 (2008) 37–46.
[72] A.F. Freitas, M.F. Mendes, G.L.V. Coelho, Thermodynamic study of fatty acids adsorption on different adsorbents, J. Chem. Thermodyn., 39 (2007) 1027–1037.
[73] J. Chang, J.C. Ma, Q. Ma, D. Zhang, N. Qiao, M. Hu, H. Ma, Adsorption of methylene blue onto Fe_3O_4/activated montmorillonite nanocomposite, Appl. Clay Sci., 119 (2016) 132–140.
[74] K. Rida, S. Bouraoui, S. Hadnine, Adsorption of methylene blue from aqueous solution by kaolin and zeolite, Appl. Clay Sci., 83 (2013) 99–105.
[75] A. Bennani, K.B. Mounir, M. Hachkar, M. Bakasse, A. Yaacoubi, Elimination of the basic methylene blue dye in aqueous solution by SAFI clay, J. Water Sci., 23 (2010) 375–388.